Journal of Ceramic Processing Research. Vol. 10, No. 6, pp. 710~715 (2009)

JOURNAL OF
Ceramic Processing Research

Microstructural characterization of multiphase GDC/NiO composites using image processing

Seung-Muk Bae[a], Kyoung-Soo Kang[b], Chu-Sik Park[b] and Jin-Ha Hwang[a,*]

[a]*Department of Materials Science and Engineering, Hongik University 72-1 Sangsu-Dong, Mapo-Gu, Seoul 121-791, Requblic of Korea*

[b]*Hydrogen Energy Research Center, Korea Institute of Energy Research, 71-2 Jang-Dong, Yuseong-Gu, Daejeon 305-343 Requblic of Korea*

Image processing was employed in combination with electron microscopy to quantitatively estimate the spatial microstructure in a multi-phase mixture used in energy-based applications. The original images were obtained using scanning electron microscopy in complementary modes, i.e. secondary electron and back-scattered electron modes. Based on the digitized and optimized images, the microstructural characterization incorporates quantitative information for each constituent, i.e. the fraction, size distribution, and contiguity. The refined image analysis procedure was applied to a mixture composed of an ionic conductor and an electronic conductor, Gd_2O_3-Doped CeO_2 and NiO. The implications of the image processing are discussed with regard to sophisticated synthesis and processing of renewable energy materials.

Key words: Image analysis, Microstructure, GDC/NiO, Renewable energy materials.

Introduction

The continual rise in the price of petroleum and the pollution issues surrounding fossil-based energy sources have contributed to an energy crisis in today's 21st century economy. Emerging sources of renewable energy offer plausible solutions to the current ecological and economic crisis. For example, the tremendous potential surrounding hydrogen-based renewable energy technology has led to the now familiar term, "the hydrogen economy." Electroceramics in particular have gained attention as a powerful candidate in the renewable energy arena, with possible applications in solid oxide fuel cells (SOFCs), water splitting materials, and oxygen transport membranes (OTMs) [1-6]. SOFCs and OTMs rely on 0-dimensional defect chemistry, specifically for ionic and electronic conductors. The SOFCs are constructed from ionic conductors, electronic conductors, and mixed conductors. OTMs currently under investigation consist of perovoskite-based mixed conductors or a combination of ionic conductors and electronic conductors [5, 6]. These two applications utilize multi-phase mixtures. The size, distribution, and amount of the respective phases influence the physical and chemical properties of the constructed article (e.g. electrical conductivity, dielectric constants, etc). An excellent overview of this technology can be found in Mchachlan *et al*'s review on electrocomposites [7]. If the pore is a major phase, then the gas-related phenomena (i.e. gas permeability and diffusivity) are critically dependent on the size and distribution microstructure of the pore phases.

This study focused on a combination of an ionic conductor and an electronic conductor, i.e., Gd_2O_3-Doped CeO_2 (GDC) and nickel oxides (NiO). The GDC/NiO mixtures are exploited as electrodes in SOFCs and as ion membranes in OTMs. Depending on the porous constituent, the porous mixture is employed either as a precursor for anodes in the SOFCs or the dense GDC/NiO composite functions as the mixed conductor in the OTMs, whose electrical behavior is based on the oxygen ion transport of the GDC and the electronic transport of the nickel. Since both approaches are based on the explicit description of the respective phase, this study focuses on the microstructural characterization of GDC/NiO with regard to image analysis. Image analysis is capable of providing quantitative explanations for the size, volume fraction, and interconnectivity of a multiphase mixture. The quantitative image analysis was applied to a series of GDC/NiO mixtures that can be used in both SOFCs and OTMs. The implications of the image analysis are discussed with regard to a systematic description of multi-phase materials.

Experimental

In order to fabricate GDC/NiO composites, mixtures were prepared using GDC (Rhodia, France) and NiO (Mitubishi, Japan). The content of the NiO was controlled as a function of the weight percent, i.e., 30, 40, 50, 60 and 70%. The necessary amount of powder for each composition was ball-milled along with a dispersing agent in a teflon jar

*Corresponding author:
Tel : +822-320-3069
Fax: +822-333-0127
E-mail: jhwang@hongik.ac.kr

using appropriate zirconia balls. The ball-milled mixtures were dried at 105 °C. After drying, the powders were pressed into 10 mm discs at a pressure of 5 MPa. The pressed specimens were heated to 1150 °C at a rate of 1 Kminute^{-1} with a hold time of 10 hours.

After heat treatment, the porous space of the sintered GDC/NiO composite specimens was filled with an epoxy resin. The molded specimens were polished to 0.25 μm using SiC abrasive papers and diamond pastes, depending upon the level of polishing. The polished surfaces were then probed by field-emission scanning electron microscopy (FESEM, JEOL, JSM-6700F, JEOL info). The images were collected in two complementary modes, as secondary electron images and back-scattered electron images. The typical acceleration voltage was fixed at 15 keV.

Refined image processing and quantitative analysis was performed using a commercial software (Version, Image-Pro, Media Cybernetics, USA). The software was used for image capturing, image optimization, and data acquisition/analysis.

Results and Discussion

Digitized images can be obtained for qualitative analyses, without numerical comparison, using a variety of analytical techniques. Among them, scanning electron microscopy has the reputation of being the most robust technique due to its visual capability and ease of operation. Scanning electron microscopy can be performed in both secondary and back-scattered electron modes. In addition, the resolution of the electron source is always increasing. Field-emission scanning electron microscopy is capable of the highest contrast and resolution as a result of its enhanced electron emission in terms of current density from the sharp-tipped electron gun. An object can be visualized in both secondary and back-scattered electron images, as shown in Fig. 1. However, the secondary electron image is only sensitive to the surface, which prevents one from differentiating the constituent phases of the multi-phase mixture [8] . However, back-scattered electron images are highly sensitive to the atomic number of the constituents. Such contrast can be exploited in order to resolve multi-phase composites into their respective constituents. The images are adapted into suitable formats that facilitate image processing. The quantified images can be obtained through a series of image conversion and data quantification steps. The image conversion includes image capturing, scale calibration, and digitized image expression based on the grey scale. The "threshold" function and noise filtering is performed in order to convert the original back-scattered images into binary images. It converted image is shown in Fig. 2, along with an originally-captured image.

Binary images should be obtained for each of the phases: in this case, GDC, NiO and the pores. The resolved images are shown in Fig. 3, using three regions to represent pores, NiO, and GDC. After this initial filtering, more detailed noise filtering is performed, specifically focusing on the

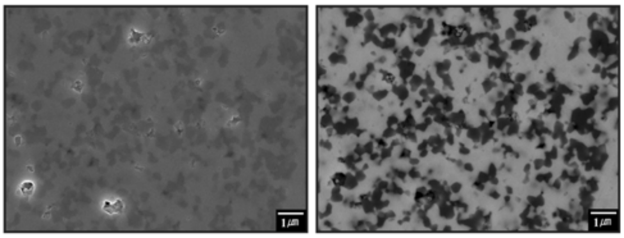

(a) (b)

Fig. 1. Typical images obtained for image processing using field-emission scanning electron microscopy. (a) secondary electron image and (b) back-scattered electron image.

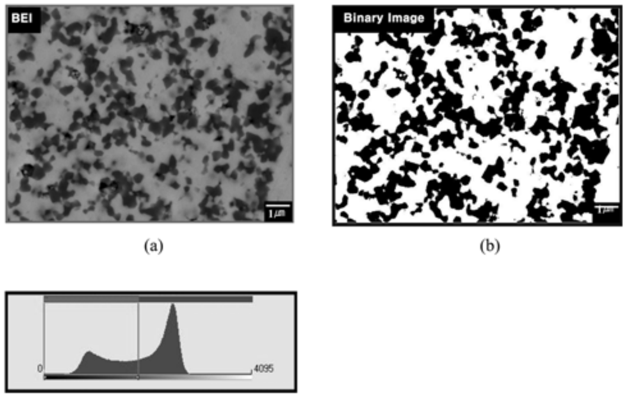

(a) (b) (c)

Fig. 2. (a) Back-Scattered electron image and (b) the converted binary image for image processing and (c) the corresponding size distribution where the horizontal and vertical axes denote the grey scale and frequency, respectively.

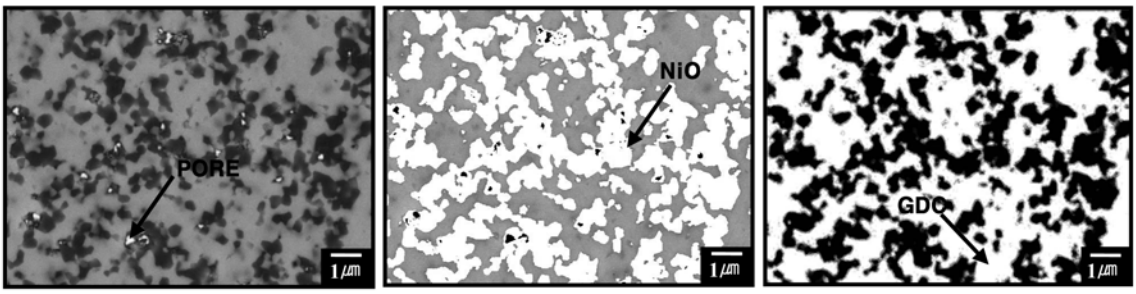

(a) (b) (c)

Fig. 3. The 1st resolved binary images after noise filtering and image optimization (a) Pore, (b) NiO and (c) GDC.

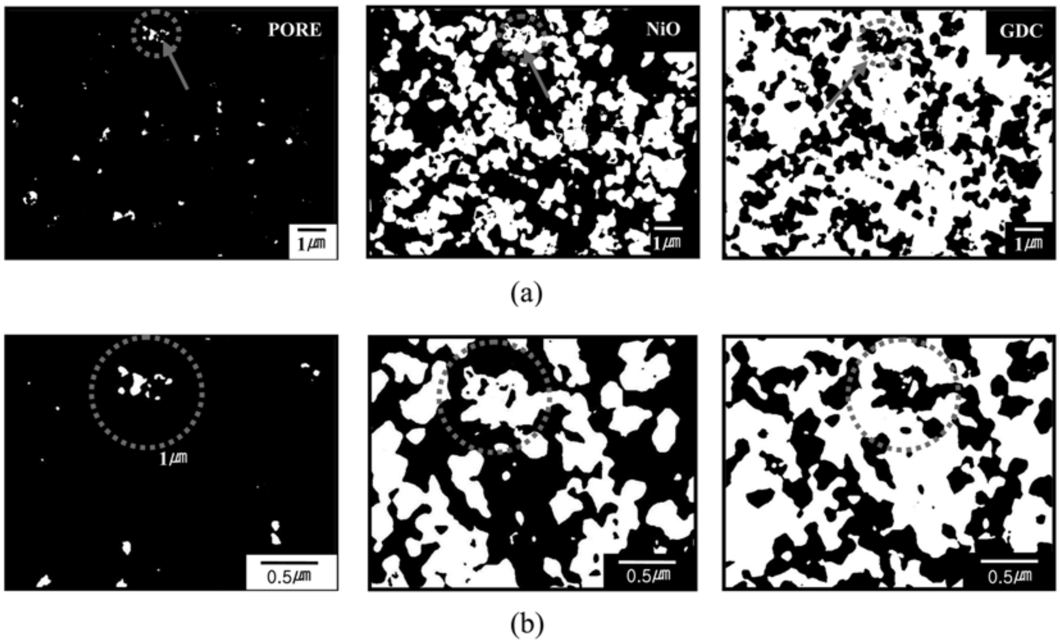

Fig. 4. (a) Binary images before (top part) and (b) after (bottom part) noise filtering near the edges of two adjacent phases.

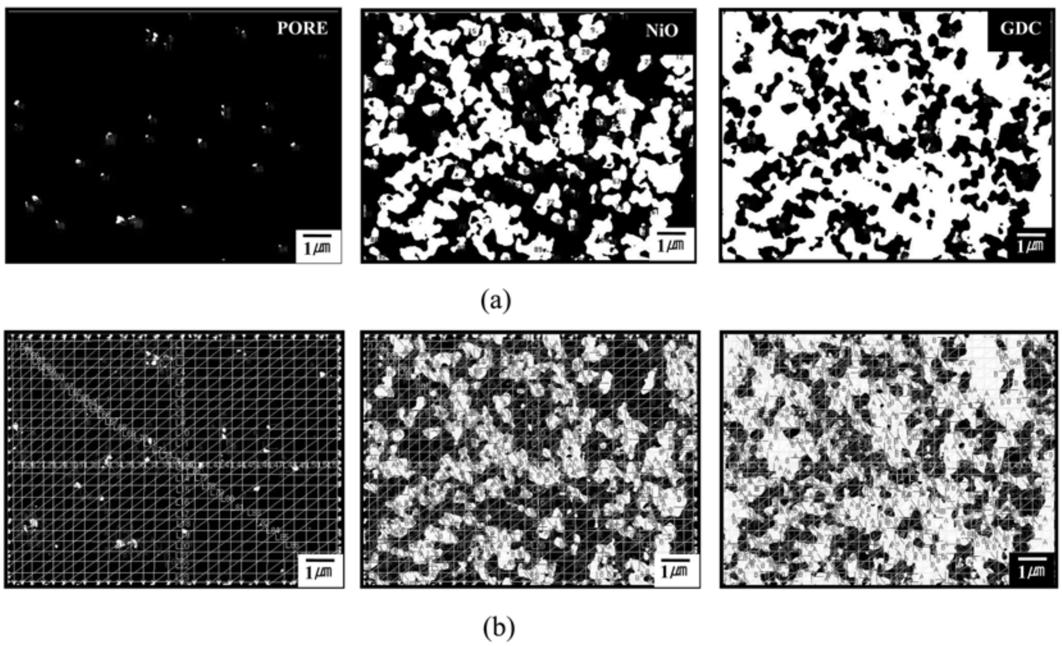

Fig. 5. Empirical procedure showing the area measurement and line intercepts for the composite materials (a) Area measurement and (b) line intercept.

edges of each phase. These small improvements in the back-scattered images can be seen in Fig. 4.

Unlike our previous study [9], the current work employs only scanning electron microscopy, specifically back-scattered electron images. An electron microscope image allows better depth-of-focus compared to that of an optical microscope, and the well-focused, high-contrast images obtained by electron microscopy are appropriate for quantitative image processing. The improved contrast of electron microscopy is appropriate for image conversion from a muliti-scale image to a binary image, as shown in Fig. 4. Furthermore, in conjunction with the availability of imaging instruments, the image acquisition and subsequent processing for electron microscopy is rather simplified.

The converted images were then used for a statistical analysis of the microstructure based on the line intercept method [10]. A total of 91 lines were drawn for the analysis of each image: 24 lines in the horizontal direction, 29 lines in the perpendicular direction, and 38 lines in the diagonal directions. The interval and reproducibility was

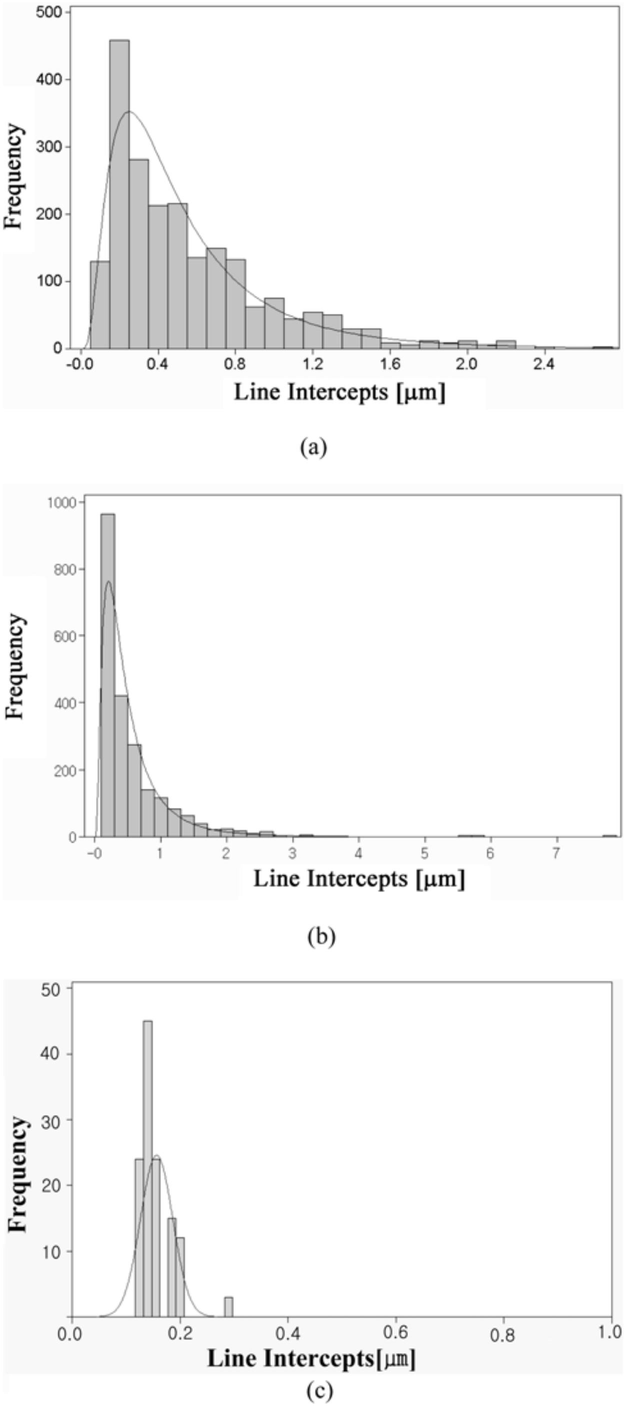

Fig. 6. The distribution of the line intercepts with regard to (a) the GDC, (b) NiO, and (c) Pore.

set using the customized macro function provided in the image analysis program. The procedures for the area measurement and line intercept are shown in Fig. 5. The resulting total areas and average line intercepts are shown in Table 1. In addition, the size distributions are shown in Fig. 6.

The statistical data shown in Table 1 and Fig. 6 were combined using statistical methodology proposed in conventional metallurgy [11-13]. The phase fraction,

Table 1. Measured surface fraction and mean line intercept (from the example) [unit : μm]

	Pores	NiO	GDC
(a) Area Fraction	0.005	0.487	0.508
(b) Mean Line Intercept	0.156	0.572	0.563

size distribution, and interconnectivity determines the overall physical properties of composite materials, e.g., electrical conductivity, dielectric constant, mechanical strength, etc. First, the measured 2-dimensional information is related to the prediction of the volume fraction of the corresponding component as follows:

$$\frac{V_i}{S_V^i} = \frac{l_i}{4} \tag{1}$$

where V_i: is the three-dimensional fraction of phase i, l_i: is the mean intercept of phase i, S_V^i is the fraction of the contact area, and V_i/S_V^i is the volume to surface area ratio of phase i.

The volume to surface area ratios are then used to calculate the interconnectivity, similar to the approach used by Lee *et al*. [9].

$$\beta_i = \frac{S_V^i}{\sum_i S_V^i} \tag{2}$$

If Eq. (1) and (2) are combined, the resultant interconnectivity of each phase can be expressed by the following:

$$\beta_{GDC} = \frac{V_{GDC} l_{NiO} l_{Pore}}{V_{NiO} l_{GDC} l_{Pore} + V_{GDC} l_{NiO} l_{Pore} + V_{Pore} l_{NiO} l_{GDC}} \tag{3}$$

$$\beta_{NiO} = \frac{V_{NiO} l_{GDC} l_{Pore}}{V_{NiO} l_{GDC} l_{Pore} + V_{GDC} l_{NiO} l_{Pore} + V_{Pore} l_{NiO} l_{GDC}} \tag{4}$$

$$\beta_{Pore} = \frac{V_{Pore} l_{GDC} l_{NiO}}{V_{NiO} l_{GDC} l_{Pore} + V_{GDC} l_{NiO} l_{Pore} + V_{Pore} l_{NiO} l_{GDC}} \tag{5}$$

The above calculation sidesteps used the practically immeasurable contact area of Eq. (1). The final interconnectivities for the 30 wt.% NiO are shown in Table 2. The interconnectivity varies depending on the fraction of each phase. The GDC phase exhibits the highest interconnectivity due to the high proportion of GDC. The samples with a combination of GDC and NiO had

Table 2. Calculated interconnectivity (or contiguity) for each component in the GDC/NiO composites. [unit : μm]

	Pores	NiO	GDC
Interconnecitivity	0.018	0.477	0.505

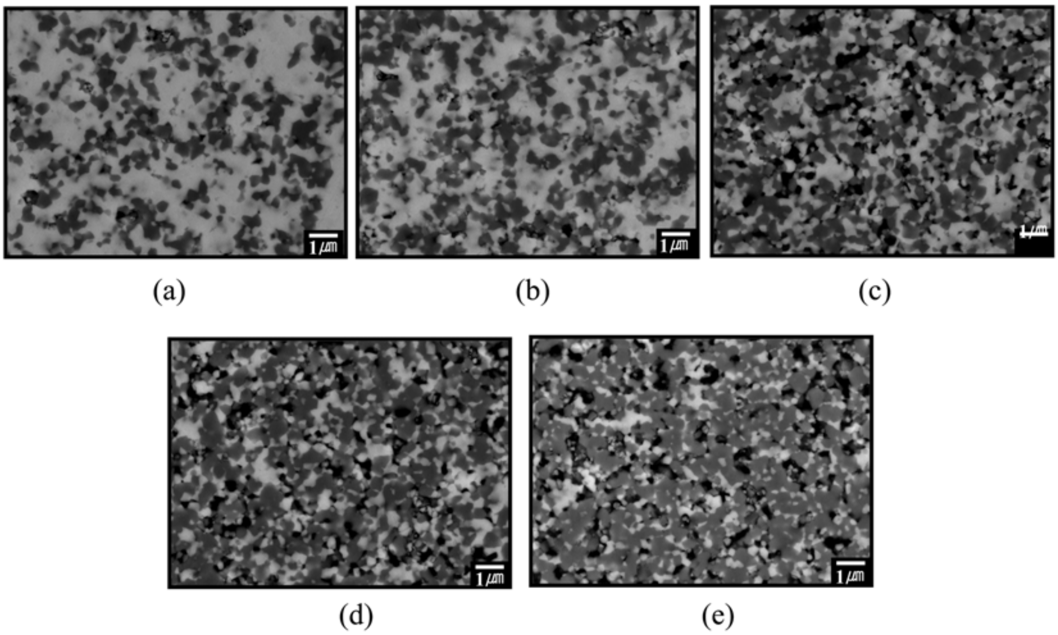

Fig. 7. Back-scattere electron images for GDC/NiO mixtures; (a) 30% NiO, (b) 40% NiO, (c) 50% NiO, (d) 60% NiO, and (e) 70% NiO.

Table 3. Summarized microstructural information for the GDC/NiO composites ranging from 30 wt.% to 70 wt.% NiO [unit : μm]

	30	40	50	60	70
Mean Line Intercept (Pore)	0.156	0.172	0.213	0.218	0.243
Mean Line Intercept (NiO)	0.572	0.452	0.318	0.289	0.266
Mean Line Intercept (GDC)	0.563	0.542	0.586	0.641	0.821
Area Fraction (Pore)	0.005	0.016	0.099	0.117	0.166
Area Fraction (NiO)	0.487	0.528	0.559	0.593	0.646
Area Fraction (GDC)	0.508	0.456	0.342	0.290	0.188
Interconnectivity (Pore)	0.018	0.044	0.166	0.176	0.204
Interconnectivity (NiO)	0.477	0.556	0.626	0.675	0.727
Interconnectivity (GDC)	0.505	0.4	0.208	0.149	0.069

a pore area fraction of 0.005 and exhibited the lowest interconnectivity value of 0.018 for the pores.

The GDC/NiO composites were chosen as the model system to first apply the image processing technique, since these composites could play a significant role in renewable energy systems. Three microstructural constituents were specified: GDC, NiO, and the pore. The NiO content of the composites ranged from 30 to 70%. (See the back-scattered images in Fig. 7.) The fraction and interconnectivity reflects the significant effect of the microstructure on the physical properties (e.g. conductivity, diffusivity, permeability, etc). The continuity of the NiO increases with an increase in line NiO content, while that of the GDC exhibits the reverse trend in its interconnectivity. The corresponding interconnectivity of the pore phases increases gently with the NiO content, i.e, from approximately zero to 0.204. This is very important for SOFCs electrodes, especially for cathodes and anodes. Furthermore, the interconnectivity information on GDC/NiO can be employed to prepare homogenized GDC/Ni composites for OTMs. The resulting information is summarized in Table 3 and Fig. 8.

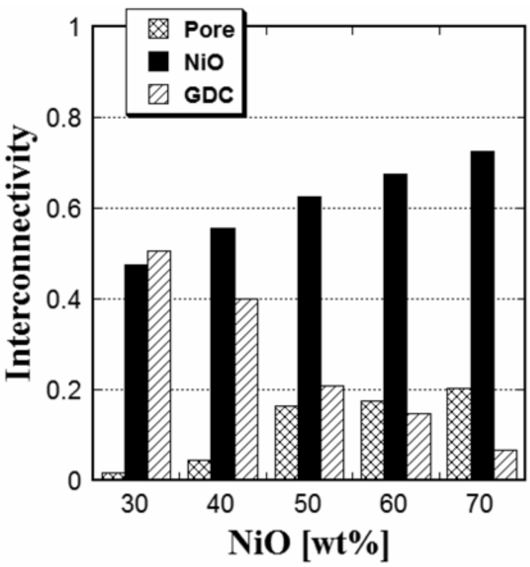

Fig. 8. Calculated interconnectivity of the component phases in the GDC/NiO composites as a function of NiO content ranging from 30 wt.% to 70 wt.%.

In summary, quantitative image processing can provide the area fraction and the line intercept of the corresponding phase from a 2-dimensional image analysis. When the empirical data from the image analysis is combined with conventional metallurgical tools, the contiguity (or interconnectivity) and volume fraction can be obtained quantitatively. These data leads to additional information about the microstructure in multi-phase composites. The quantification of image processing can lead to an optimization of i) electrodes in terms of delivery of reactants and removal of reactants in SOFCs and ii) OTMs in terms of balanced electrochemical reactions through appropriate control of ionic and electronic conductions in producing hydrogen.

Conclusions

Image processing was attempted in conjunction with scanning electron microscopy with the aim of quantifying the microstructural properties in energy-oriented composites, i.e. GDC/NiO mixtures. Back-scattered electron images were employed in digitizing the microstructural images. The GDC/NiO composites were analyzed in terms of the volume fraction, size, and distribution, along with the interconnectivity of the corresponding constituents, i.e. GDC, NiO, and pore. The contiguity of GDC decreases and that of NiO increases with increasing amounts of NiO. The contiguity of the pores increases gently with respect to variation in NiO content.

Acknowledgements

This Research was performed for the Hydrogen Energy R&D Center, one of the 21st Century Frontier R&D Program, funded by the Ministry of Education, Science, and Technology of Korea.

References

1. N.Q. Minh, J. Am. Ceram. Soc. 76[3] (1993) 563-588.
2. J.T. Brown, Energy 11 (1986) 209-229.
3. S. Abanades and G. Flamant, Solar Energy 80 (2006) 1611-1623.
4. A. Steinfeld, Solar Energy, 78 (2005) 603-615
5. H. Naito and H. Arashi, Solid State Ionics 79 (1995) 366-370.
6. U. Balachandran, T.H. Lee and S.E. Dorris, International Journal of Hydrogen Energy 32 (2007) 451-256.
7. D.S. McLachlan, M. Blaczkiewicz and R.E. Newnham, J. Am. Ceram. Soc. 73[8] (1990) 2187-2203.
8. C.R. Brundle, C.A. Evans, Jr. and S. Wilson in Encyclopedia of Materials Characterization edited by (Manning Publications Co., 1992) p. 57.
9. K.-R. Lee, S.H. Choi, J. Kim, H.-W. Lee and J.-H Lee, Journal of Power Sources, 140 (2005) 226-234.
10. D. Simwonis, F. Tietz and H. Tagawa, Solid State Ionics 132 (2000) 241-251
11. K.B. Alexander, P.F. Becher, S.B. Waters, A. Bleier, Journal J. Am. Ceram. Soc. 77[4] (1994) 939-946.
12. C.S. Smith, L. Guttman, Trans. Metall. Soc. AIME 197 (1953) 81-87.
13. J.W. Cahn and J.E. Hilliard, Trans. Metall. Soc. AIME (1959) 759-761.